TEAM 2018, *Oct. 15 - 18, 2018, Wuhan, China*

Strength Evaluation of Cross Deck for High-speed Catamaran Coupling with Seakeeping Simulation

Chien-Ting SUN*[1], Po-Kai LIAO[1], Chun-Ta LIN[1], Ya-Jung LEE[2]

1) R/D Section, Research Department, CR Classification Society
2) Department of Engineering Science and Ocean Engineering, National Taiwan University
* e-mail: ctsun@crclass.org

Abstract
The structural scantling of High Speed Craft (HSC) of length less than 50 m is mostly driven by the local scantling requirements related to the design wave pressure and acceleration. However, for the case of catamaran-type HSC such as the passenger ship considered in this study, the Class rules require also to assess the Cross-deck structural strength under Beam and Quartering seas. In this study, the wave pressure distribution and the associated ship motions were obtained by seakeeping simulation using RANS formulation Computational Fluid Dynamic (CFD) method in time domain. The pressure distribution was then transferred to the Finite Element (FE) model through a high order interpolation method called the Reproducing Kernel Particle Method (RKPM). Finally, coupled hydro-structure simulations were conducted on the considered HSC catamaran under Beam and Quartering seas, and the obtained structural stresses were compared to those produced by simplified load application derived from the rules loads.

Keyword: High Speed Craft, Catamaran, Fluid-Structure Interaction, Seakeeping, Structure Strength

1. INTRODUCTION

The structural scantling of High Speed Craft (HSC) of length less than 50 m is mostly driven by the local scantling requirements related to the design wave pressure and acceleration. However, for the case of catamaran-type HSC such as the passenger ship considered in this study, the Class rules require also to assess the Cross-deck structural strength under Beam and Quartering seas. Various approaches are proposed by researchers and Classes to simplify the structural strength evaluation and thus reduced the time to spend for the analysis while keeping an eye on the accuracy and thus the safety. [1]-[4] developed strategies to simplify the structural modeling of the catamaran by neglecting the contribution of the superstructure to the strength and by using Beam finite elements to model the Cross-deck structure and the Floats. However, for more accuracy, the present study employed a detailed model of the ship structure including the superstructure using Shell finite elements. Besides, the rules often recommends simplified loads application representing the wave pressure distribution as series of concentrated forces acting along floats and resulting in the design global loads provided by the rules in terms of transverse bending moment for the Beam sea and pitch connection moment for the Quartering sea. However, this simplified loads application ignores the reality of the wave dynamic pressure distribution and its evolution in the time, and it disregards the associated inertia loads induced by the ship motions. Therefore, in this study seakeeping analyses in time-domain were also conducted to produce the wave pressure distribution and the associated ship motions to be applied on the structural FE model using a Fluid-Structure Interaction scheme.

Various procedures are nowadays available to address the Fluid-Structure Interaction (FSI) through numerical analyses that imply various levels of complexity. The most comprehensive FSI procedures, so called monolithic, employ multiphysic software packages that enable solving the fluid and structure problems synchronously. However, the most popular FSI procedures are referred as partitioned procedures that solve separately the fluid and structure problems in two different steps conducted in parallel by employing, usually, two different software packages, respectively Computational Fluid Dynamic (CFD) and Finite Element Analysis (FEA). The present study employed a partitioned procedure to simulate the Fluid-Structure Interaction for which the fluid problem, so called seakeeping analysis, was solved using the RANS formulation CFD software STAR CCM+, and the structural analysis was carried out using NX NASTRAN. In addition, this study adopted a 'one-way' FSI approach for which the CFD loads are transferred to the FE model for structural analysis, but the structural deformations are not transferred back to the hydro-model that is considered as rigid. This study also adopted a quasi-static approach to solve the structural problem for which each step is computed independently from the previous by simply considering the hydrodynamic loads and the associated motions and accelerations of the ship produced by the CFD at a given time-step. Those simplifications are deemed reasonable with respect to the small and relatively slow structural deformations that will not significantly affect the hydrodynamic and the dynamic structural responses. A high-order kernel-based

approximation method was employed to map accurately the hydrodynamic pressure from the fluid model to the structural model.
This study evaluated the Cross-deck structural strength of a catamaran-type passenger High-Speed Craft (HSC). Tables 1 and 2 list the main particulars of the ship and of its Cross deck structural arrangement.
The first section presents the seakeeping computations including the governing equations, computational domain, and wave conditions. The second section presents the mapping process and the interpolation method, namely reproducing kernel particle method (RKPM). The last section compares the results of the structure analyses obtained using seakeeping simulations to those produced by the simplified loads application derived from the rules [5].

Table 1. *Ships main particulars.*

	HSC
Length at the water line, L_{wl}	39.5 m
Breadth, B	10.0 m
Float width amidship, B_W	2.6 m
Depth, D	3.4 m
Draft amidship, d	1.38 m
Service speed, V_s	25 knt
Design vertical acceleration, a_{cg}	0.68 g's

Table 2. *Design loads and Cross-deck structural arrangement.*

	HSC
Rules transverse bending moment, M_{bt}	1647 kN.m
Rules pitch connection moment, M_{tt}	5576 kN.m
Cross-deck height, H_{CD}	0.8 m
Cross deck width between Floats, S	3.4 m
Transverse frame spacing (avg.), w	1.0 m
Strength deck thickness, $t_{s\text{-}deck}$	2 mm
Wet deck thickness, $t_{w\text{-}deck}$	6 mm

2. SEAKEEPING COMPUTATIONS BY COMPUTATIONAL FLUID DYNAMIC METHOD

In STAR-CCM+, the Navier-Stokes equations are solved to model the fluid flow around the ship body. This study utilizes the Reynolds Averaged Navier Stokes Equations approach (RANS). The mean mass and momentum transport equation can be written as follows:

$$\frac{\partial \rho}{\partial t} + \nabla \cdot \left[\rho\left(\overline{\mathbf{v}} - \mathbf{v}_g\right)\right] = 0 \tag{1}$$

$$\frac{\partial}{\partial t}\left(\rho \overline{\mathbf{v}}\right) + \nabla \cdot \left[\rho \overline{\mathbf{v}}\left(\overline{\mathbf{v}} - \mathbf{v}_g\right)\right] = -\nabla \cdot \overline{p}\,\mathbf{I} + \nabla \cdot \left(\mathbf{T} - \rho \overline{\mathbf{v}'\mathbf{v}'}\right) + \mathbf{f}_b \tag{2}$$

Where ρ is the density, $\overline{\mathbf{v}}$ and $\overline{p}$ are the mean velocity and pressure respectively, $\mathbf{v}_g$ is the reference frame velocity relative to the laboratory frame, $\mathbf{I}$ is the identity tensor, $\mathbf{T}$ is the stress tensor, and $\mathbf{f}_b$ is the resultant of the body forces (such as gravity and centrifugal forces).

Computational Domain and Boundary Conditions

In STAR-CCM+, the computational domain for seakeeping analysis in regular waves was produced using an overset mesh region that follow the motions of the full-scale High-Speed catamaran model over the static background mesh region of the whole fluid domain. The settings of the seakeeping simulation were validated in [6] for a similar catamaran-type HSC under Head sea condition for which the model test basin were available.
A general view of the computation domain with the catamaran hull model and the notations of selected boundary conditions are depicted in Fig. 1. It illustrates that a velocity inlet boundary condition was set in the positive X-direction and negative Y-direction, where incident regular waves were generated. To work in with the movement of the computational domain, the negative X-direction is also modeled as a velocity entry. The top and bottom boundaries were both selected as slip-wall. The selection of boundary conditions from any appropriate combination would not affect the flow results significantly, provided that they are placed far enough from the ship hull, such that the flow is not disturbed by the presence of the body. Also, the pressure outlet boundary condition was set in the positive Y-direction since it prevents backflow from occurring and wave reflection.

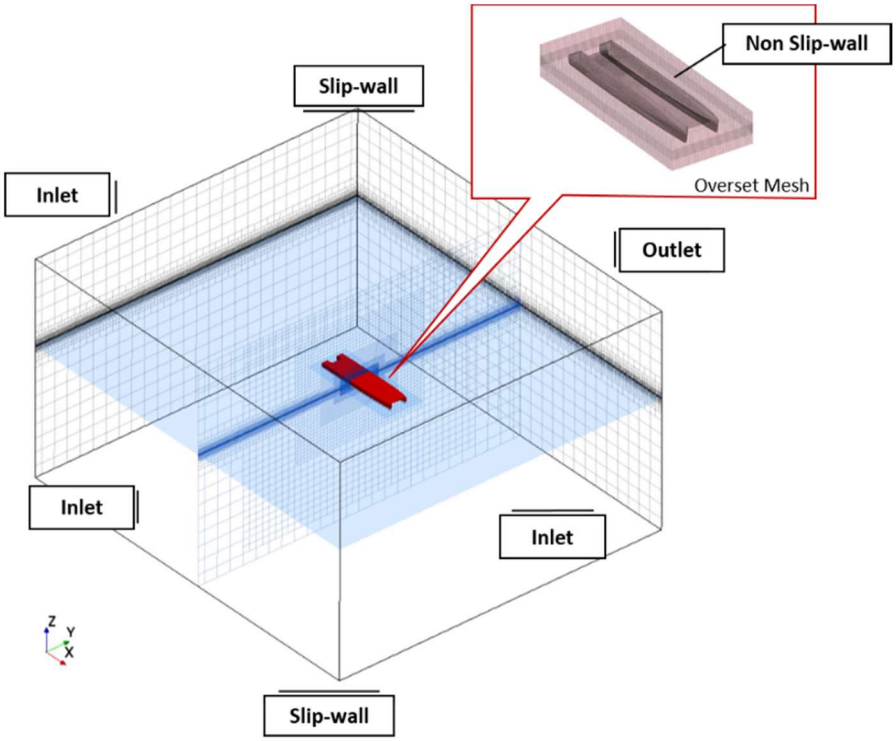

Fig. 1 *General view of the background and overset mesh regions, and the applied boundary conditions.*

Wave Conditions

This study simulated by CFD the full-scale catamaran operating at 25 knots in waves modeled using a first order VOF scheme and a periodic sinusoidal wave profile consistently with the assumed deep water condition. Fig. 2 shows the two wave headings conditions simulated by CFD. For the Beam sea, the wave length was set to 20 m and corresponds to twice the ship width in order to maximize the roll motion and thus the transverse bending moment in line with the rules technical background. For the Quartering sea, the 14.5 m wave length was obtained by Eq. (3) together with the 104° wave heading according to [7] in order to maximize the pitch connection moment in line with the rules technical background. The height was arbitrarily set to 0.8 m to limit the motions and thus the computation time of the seakeeping analyses while getting realistic wave steepness related to the ship dimension.

$$L_{WQ}=\frac{2L_{wl}B}{\sqrt{L_{wl}^2+B^2}} \tag{3}$$

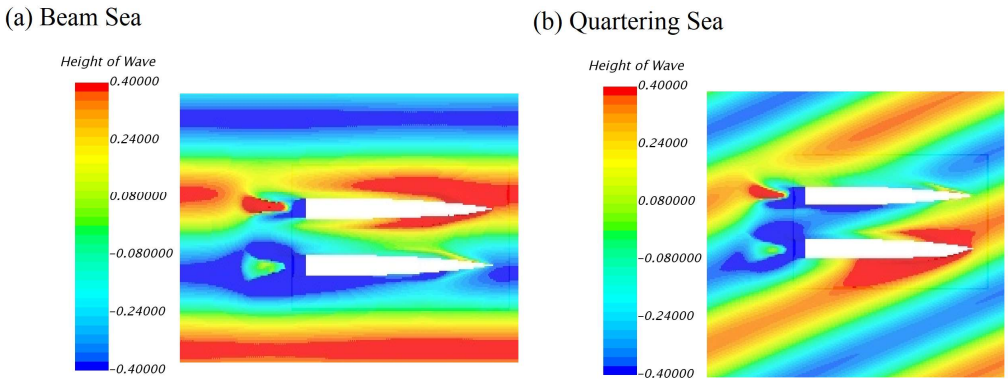

Fig. 2 *Wave conditions simulated by CFD for (a) Beam sea and (b) Quartering sea.*

3. PRESSURE MAPPING PROCESS

This study developed a mapping process to transfer the wave pressure distribution from the hydro-model as computed by CFD analysis to the structural FE model. The order of interpolation can be adjusted easily.

Reproducing Kernel Approximation

The interpolating method is called the Reproducing Kernel Particle Method (RKPM) [8], and it is a kernel based method. In the RKPM, the approximation of pressure field can be presented as：

$$P^{struc}(\mathbf{x}) = \sum_{I=1}^{NP} \Psi(\mathbf{x}, \mathbf{x}-\mathbf{x}_I) P_I^{hydro} \tag{4}$$

where $P^{struc}(\mathbf{x})$ is the pressure on location $\mathbf{x}$ of structural mesh, and P_I^{hydro} is the pressure on location $\mathbf{x}_I$ of hydro-mesh. Index I means I-th pressure points on the hydro-mesh, and NP is the total number of pressure points. In Eq. (4), $\Psi(\mathbf{x}, \mathbf{x}-\mathbf{x}_I)$ is the shape function of I-th pressure points, and it can be written as:

$$\Psi(\mathbf{x}, \mathbf{x}-\mathbf{x}_I) = C(\mathbf{x}; \mathbf{x}-\mathbf{x}_I)\phi_a(\mathbf{x}-\mathbf{x}_I) \tag{5}$$

where $C(\mathbf{x}; \mathbf{x}-\mathbf{x}_I)$ is the correction function that controls the order of approximation, and $\phi_a(\mathbf{x}-\mathbf{x}_I)$ is the kernel function that guarantees the continuity and smoothness of the shape function. In this study, the correction function is a polynomial function, and the kernel function is cubic B-spline function.

Pressure Mapping Process

The CFD fluid pressure distribution on the two floats was output as series of pressure point, as represented in Fig. 3. The pressure was then transferred on the structural mesh using the centroid $\mathbf{x}_J$ of the Shell elements, and Eq. (4) becomes:

$$P^{struc}(\mathbf{x}_J) = \sum_{I=1}^{NP} \Psi(\mathbf{x}_J, \mathbf{x}_J-\mathbf{x}_I) P_I^{hydro} \tag{6}$$

Fig. 4 presents the pressure mapping process. At the initial state, the shape functions $\Psi(\mathbf{x}_J, \mathbf{x}_J-\mathbf{x}_I)$ are determined to represent the relation between pressure points and middle points. Then, at every time step, the Eq. (6) is computed to produce the pressure approximation on structural mesh.

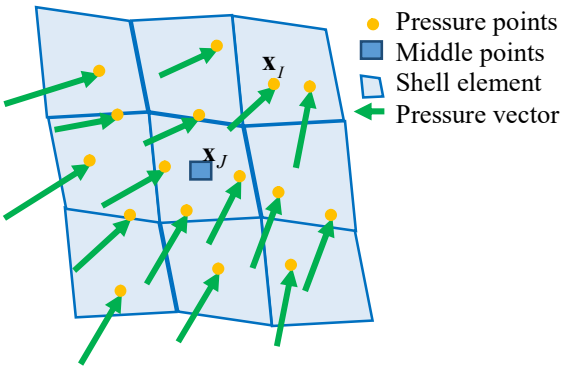

Fig. 3 *Interface of hydro-mesh and structural mesh.*

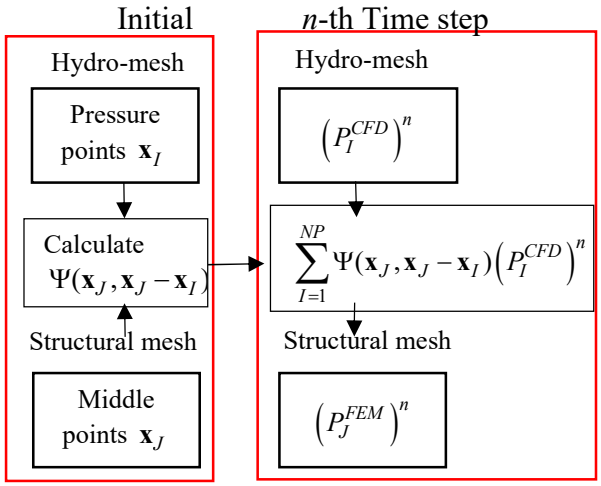

Fig. 4 *Pressure mapping process.*

4. STRUCTURAL ANALYSES

Structural analyses were conducted using a full ship FE model made of shell elements with a global mesh size of one tenth of frame spacing by one half of stiffener spacing. For comparison, the FE model was loaded using the CFD loads produced through the seakeeping analysis and the simplified load distribution derived from the rules [5].

Structural Analyses using seakeeping loads

The comparisons of pressure distribution between CFD and FEM model in different time and seakeeping simulation are illustrated in Fig. 5 and Fig. 6 . This study adopted the 'one-way' FSI approach described in introduction, so that 23 time steps of static FEA were computed over one wave period. The static structural FEA requires boundary conditions, to prevent the singularity of the stiffness matrix. However, the load application on the FE model must be balanced so that the reaction forces at those constrained nodes remain negligible.

Fig. 7 and Table 3 present the boundary conditions applied for the Beam and Quartering seas load cases. Fig. 8 shows the FE results in terms of transverse stresses (i.e. global Y-axis) for both the Beam and the Quartering seas at the time step when the transverse bending and the pitch connection bending, respectively, were the greatest. Here, the wet deck is the most highly stressed region in the whole ship. In addition, it worth noting that, although the Von Mises stresses relates directly to the structural strength criterion, here, the transverse stresses were preferred for display as they

reflect the structural response to the transverse bending moment and pitch connection moment that the ship undergoes during Beam and Quartering seas, respectively. It can be observed that the transverse stress magnitude is much smaller than the material limit of ~130 N/mm^2, so that the structural strength will not be exposed under those two wave conditions.

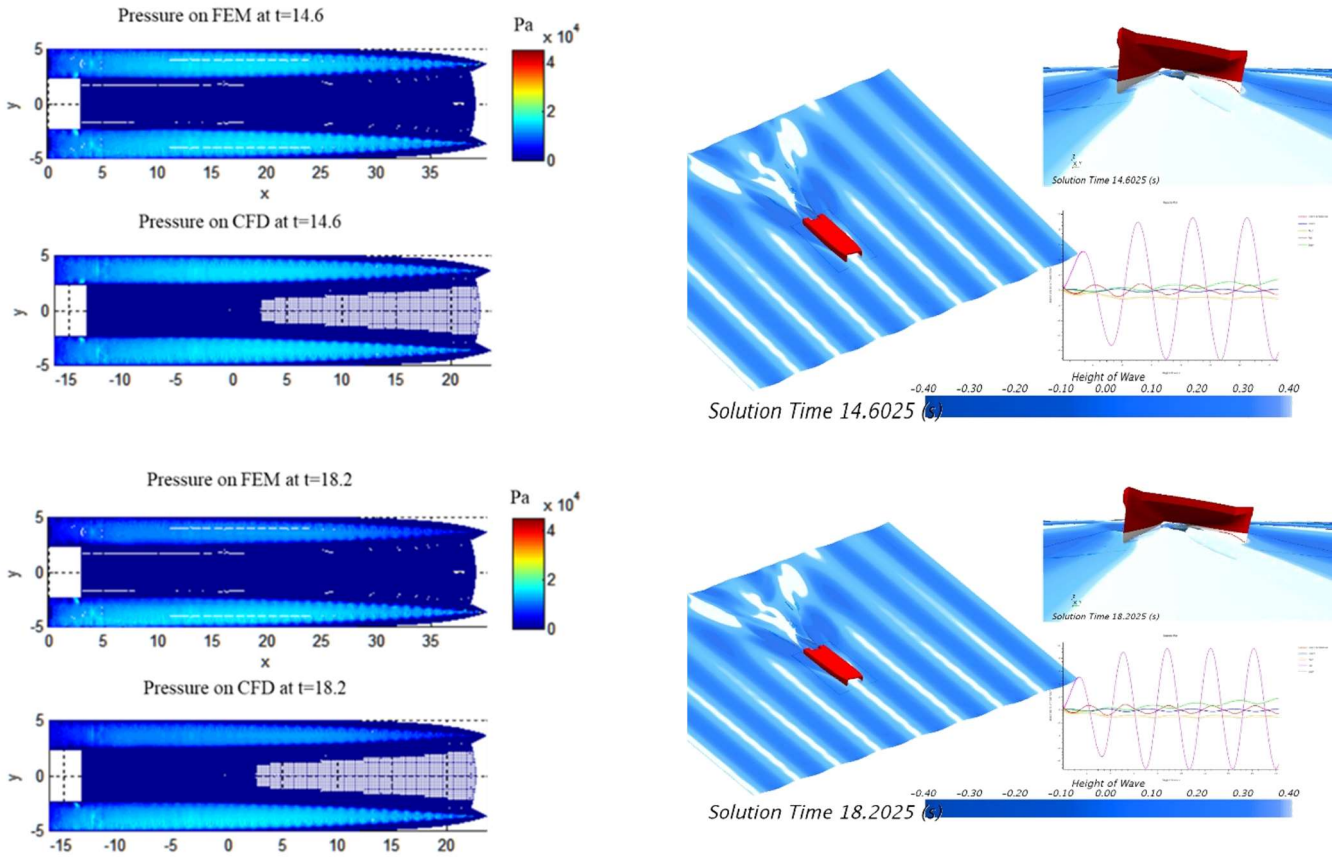

Fig. 5 *Comparisons of pressure distribution at 14.6 sec and 18.2 sec for Beam sea.*

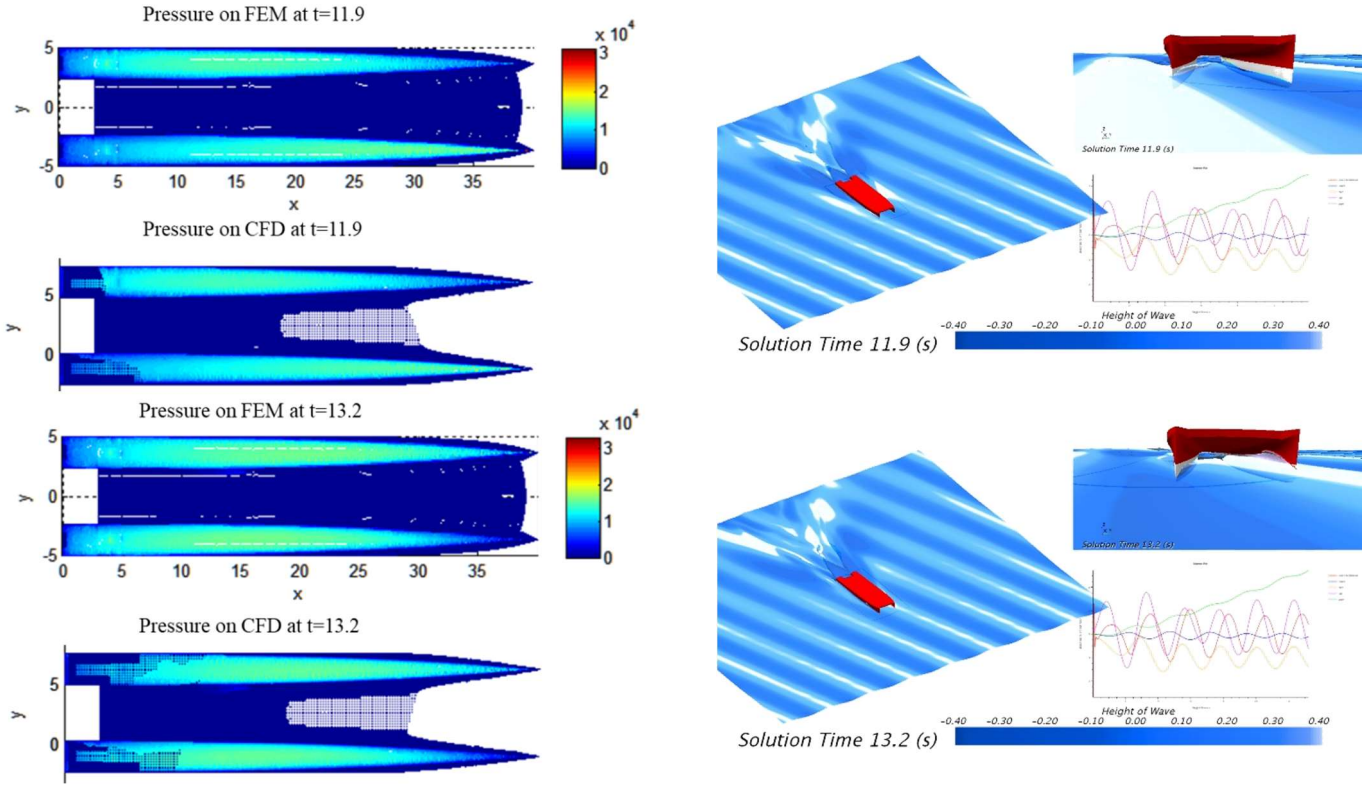

Fig. 6 *Comparisons of pressure distribution at 11.9 sec and 13.2 sec for Quartering sea.*

Table 3. *Boundary condition settings.*

	UX	UY	UZ	RX	RY	RZ
CL_A		☒	☒			
CL_B		☒	☒			
CL_C	☒		☒			

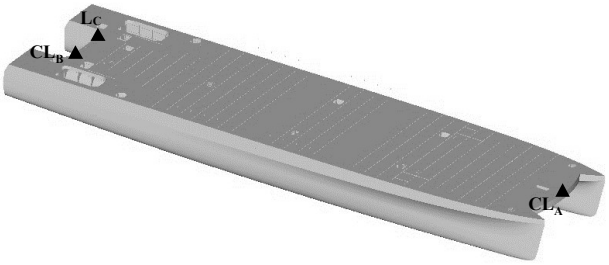

Fig. *7 Locations of Boundary conditions.*

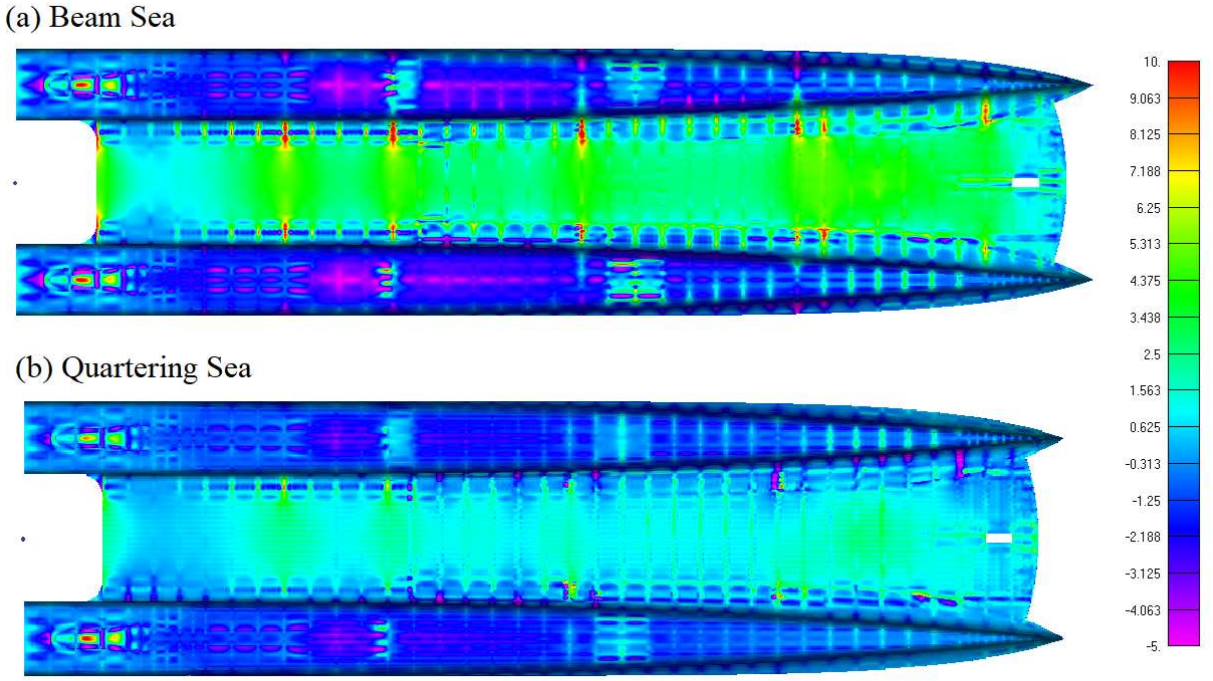

Fig. 8 *Transverse stresses on wet deck produced by FEA with seakeeping loads for Beam and Quartering seas.*

Structural Analyses using simplified load application

For the Beam sea, the rules design transverse bending moment M_{bt} in the Cross-deck was reproduced by applying nodal forces at the mid-draft in way of the transverse web frames, as shown in Fig. 9. The uniform horizontal line pressure in force per unit length q_y was calculated using Eq. (6). For the Quartering sea, the rules design pitch connection moment M_{tt} in the Cross-deck was reproduced by applying nodal forces at the keel line in way of the transverse web frames. Fig. 10 shows the load application on the FE model with the nodal forces taken upwards for the aft half of starboard float and the fore half of port-side float, and downwards for the fore half of starboard float and the aft half of port-side float. The uniform vertical line pressure in force per unit length q_z was calculated using Eq. (7).

$$q_y = \left[M_{bt} / (z_{NA} - d/2)\right] / L_{wl} \tag{6}$$

$$q_z = 4M_{tt} / L_{wl}^2 \tag{7}$$

where z_{NA} is the vertical coordinate of the Cross-deck's neutral axis.

The boundary conditions for both Beam and Quartering seas load cases are presented in Table 4 and Fig. 11. Fig. 12 shows the FE results in terms of transverse stresses (i.e. global Y-axis) for both load cases. Here, the wet deck is the most highly stressed region in the whole ship. In addition, it worth noting that, although the Von Mises stresses relates directly to the structural strength criterion, here, the transverse stresses were preferred for display as they reflect directly the structural response to the transverse bending moment and pitch connection moment that the ship undergoes during Beam and Quartering seas respectively. It can be observed that the transverse stress magnitude is much smaller than the material limit ~130 N/mm^2, so that the structural strength will not be exposed under those two wave conditions.

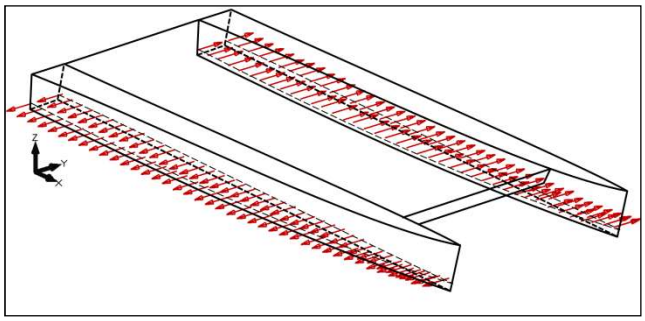

Fig. 9 *Simplified load application for Beam sea.*

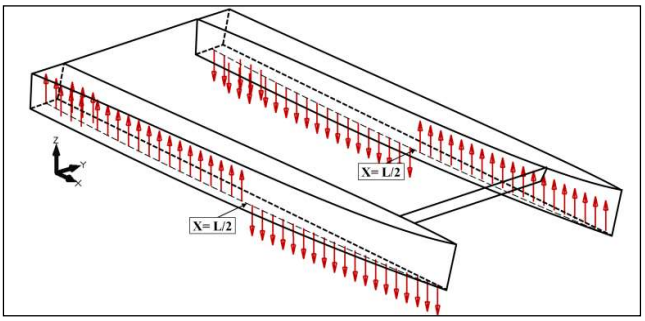

Fig. 10 *Simplified load application for Quartering sea.*

Table 4. *Boundary condition settings.*

	UX	UY	UZ	RX	RY	RZ
CL_A	X	X	X			
CL_B		X				
CL_C		X	X			

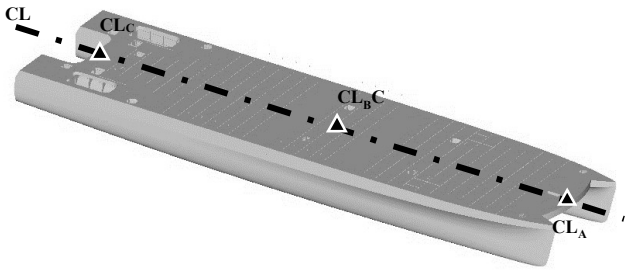

Fig. 11 *Locations of Boundary conditions.*

(a) Transverse bending

(b) Pitch connecting moment

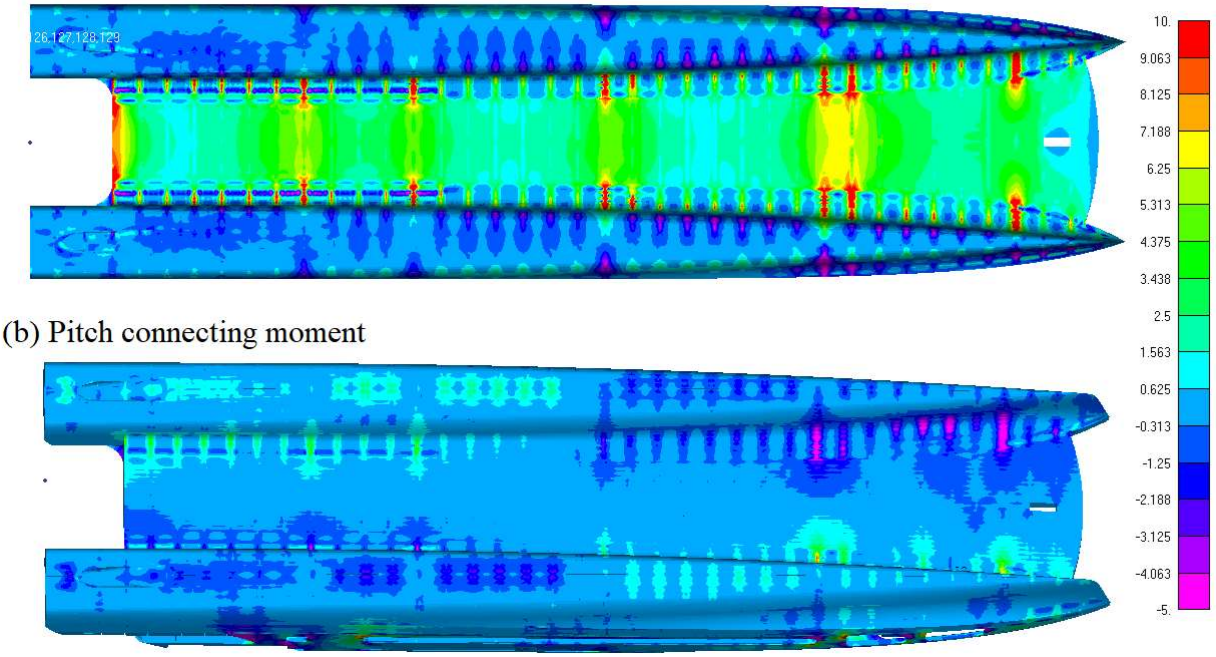

Fig. 12 *Transverse stresses on wet deck produced by FEA with simplified loads for Beam and Quartering seas.*

Comparison of FE results

Fig. 13 and Fig. 14 present the normalized transverse stress (i.e. global Y-direction) on the wet deck respectively taken along the centreline and along the float connection, for the Beam sea load case produced using the seakeeping loads and by the simplified loads. The magnitude of the transverse stress produced by both load application approaches cannot be compared since the global transverse bending moment obtained by seakeeping analysis was not calibrated on the rules design loads. However, the trend of the normalized transverse stress distribution along the ship length can provide interesting information. Indeed, it can be observed that both simplified and seakeeping loads resulted in similar normalized transverse stress distribution along both the centreline and the float connection, which

would mean that once the global load produced by both approaches would be unified, the level of transverse stress would be similar.

Likewise, Fig. 15 and Fig. 16 present the normalized transverse stress (i.e. global Y-direction) on the wet deck respectively taken along the centreline and along the float connection, for the Quartering sea load case produced using the seakeeping loads and by the simplified loads. Again, the magnitude of the transverse stress produced by both load application approaches cannot be compared since the global pitch connection moment obtained by seakeeping analysis was not calibrated on the rules design loads. However, the trend of the normalized transverse stress distribution along the ship length can provide interesting information. Indeed, it can be observed that both simplified and seakeeping loads resulted in similar normalized transverse stress distribution along both the centreline and the float connection, which would mean that once the global load produced by both approaches would be unified, the level of transverse stress would be similar.

Further efforts are thus needed to unify the global loads produced by both load application approaches before to confirm that the simplified load application approach is as accurate and safe as it is practical in comparison to the realistic seakeeping loads.

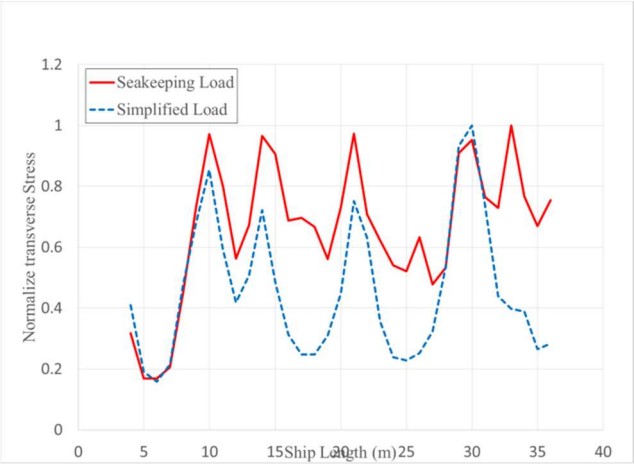

Fig. 13 *Normalized transverse stress on the wet deck at the Centerline under Beam sea.*

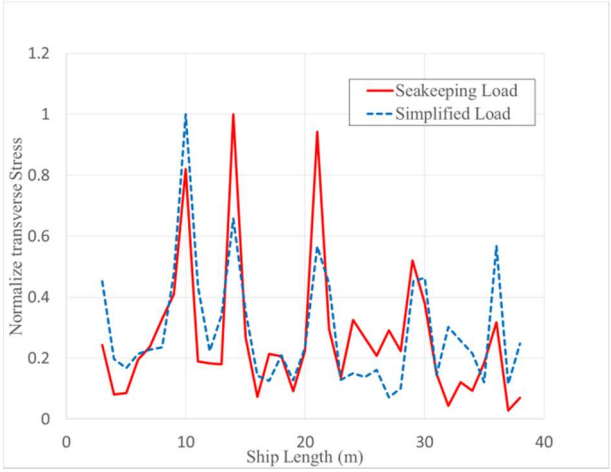

Fig. 14 *Normalized transverse stress on the wet deck at the float connection under Beam sea.*

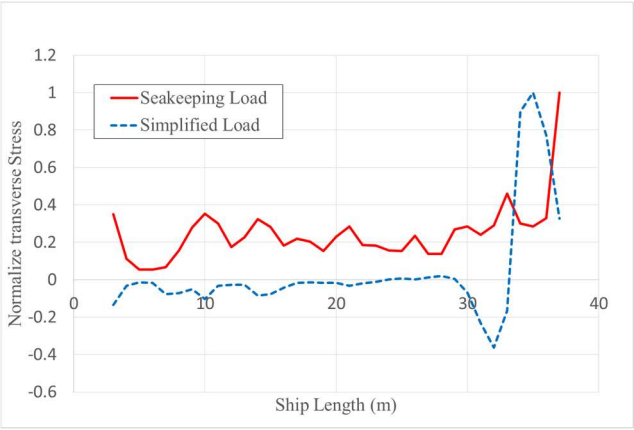

Fig. 15 *Normalized transverse stress on the wet deck at the Centerline under Quartering sea.*

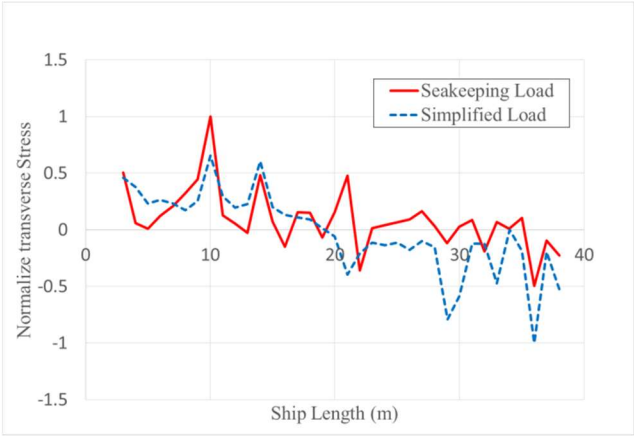

Fig. 16 *Normalized transverse stress on the wet deck at the float connection under Quartering sea.*

CONCLUSIONS

This study compared the structural response of a high speed catamaran under Beam and Quartering seas through finite element analysis using CFD loads directly computed by RANS formulation seakeeping analysis and using simplified load derived from the rules. The seakeeping loads were obtained for a wave which the length was in agreement with the rules loads assumptions, but the height was arbitrarily defined, so that the magnitude of the transverse bending moment and that of the pitch connection moment for the Beam and the Quartering seas, respectively, could not be compared. Likewise, the structural response and especially the transverse stresses on the wet deck produced by both load application approaches could not be compared. However, the distribution of the normalized wet deck transverse stress along the centreline and the float connection showed obvious similarities for both load application approaches. Therefore, further efforts are still needed to unify the global loads produced by both load application approaches before to confirm that the simplified load application approach is as accurate as it is practical in comparison to the realistic but laborious CFD loads directly computed by RANS formulation seakeeping analysis.

ACKNOWLEDGEMENTS

This project is funded by the Ministry of Science and Technology (MOST) (107-2221-E-002-088-MY2)

REFERENCES

[1] Liao PK, Quemener Y, Syu YC, Chen KC, & Lee YJ, Validation of Practical Approaches for the Strength Evaluation of High-speed Catamaran under Beam and Quartering Seas, *The 31st Asian-Pacific Technical Exchange and Advisory Meeting on Marine Structure,* (2017)

[2] BV Classification Society, Rules for the Classification of High Speed Craft, (2002)

[3] Zheng J., Xie W., YangL.,&Yao-wu H., Simplified Calculation of Catamaran Cross-Deck Structural Strength, *Chinese Journal of Ship Research*,4, (2010), 36-39.

[4] Yasuhira Y., Hiroyasu T., On simplified method to analyze the cross-deck floor strength of catamaran subjected to pitch connecting moment, *Journal of the Society of Naval Architects of Japan*,191,(2002),247-254.

[5] CR Classification Society, Rules for the Construction and the Fabrication of High Speed Craft, (2017).

[6] Lin CT, Lin TY, Lin CW, Hsieh YW, Lu L and Hsin CY, Investigation of the Seakeeping Performance of Twin Hull Vessels by Different Computational Methods, *10th International Workshop on Ship and Marine Hydrodynamics*, (2017)

[7] BV Classification Society, Hull Structure and Arrangement for the Classification of Cargo Ships less then 65 m and Non Cargo Ships less than 90 m, (2014)

[8] Liu WK, Jun S, Zhang YF. Reproducing Kernel Particle Methods. Int J Numer Methods Fluids, (1995), 1081-106.